3.4 THE EFFECT OF THE STABILITY OF THE ATMOSPHERIC BOUNDARY LAYER ON THE COASTAL UPWELLING OVER THE CALIFORNIA COAST

Adam Kochanski and Darko Koracin*
Desert Research Institute, Reno, Nevada

Clive Dorman[12]
[1]Scripps Institution of Oceanography, San Diego, California
[2]San Diego State University, San Diego, California

Gordana Beg Paklar
Institute of Oceanography and Fisheries, Split, Croatia

1. INTRODUCTION

The wind stress over the ocean is a crucial parameter driving the ocean circulation. On the other hand, this circulation affects also the sea surface temperature which influences the wind stress. The simplest approach leading to the evaluation of the wind stress is based on the bulk formula. One of the most extensively used is the one proposed by Large and Pond (1981). According to this formula, the drag coefficient is computed solely based on the wind speed and air density, which makes the computation easy, and applicable also for prognostic purposes when the wind speed is forecasted by the atmospheric model. However, this convenient methodology has its limitations. This bulk formula applies to the neutral atmospheric stratification. Therefore, the effect of stability on the wind stress can not be captured by this formula, nor can the effect of the spatial variations of the atmospheric stability on the wind stress curl. For the computation of the stability-corrected wind stress, one can use the TOGA-COARE algorithm developed by Fairall et al. (1996a,b). However, since the sea surface temperature is required for this computation, this methodology in the prognostic purposes requires data from an ocean model. At this point, the question on how important the stability effect can be in terms of evaluation of the wind stress and wind stress curl arises, as well as how the stability-induced wind stress and wind stress curl variations affect ocean upwelling. We also want to investigate how including the atmospheric stability in the wind stress computation based on MM5 data affects the results of the ocean model forced by the atmospheric model.

2. METHODOLOGY

As a source of the basic meteorological data we used The Fifth-Generation NCAR / Penn State Mesoscale Model (MM5) version#3. The analyzed 9km resolution domain (127x103) covers the area between 32˚ and 42˚ north and 116˚ and 126˚ degrees west - see Fig.1. For the analysis of the ocean response to a changed atmospheric forcing we used the Princeton Ocean Model (POM) released on 03-05-2006. In order to avoid problems with interpolating data between the atmospheric and ocean model domains, the POM model domain was set in a way that the location of the POM grid points matched the location of MM5 grid points.

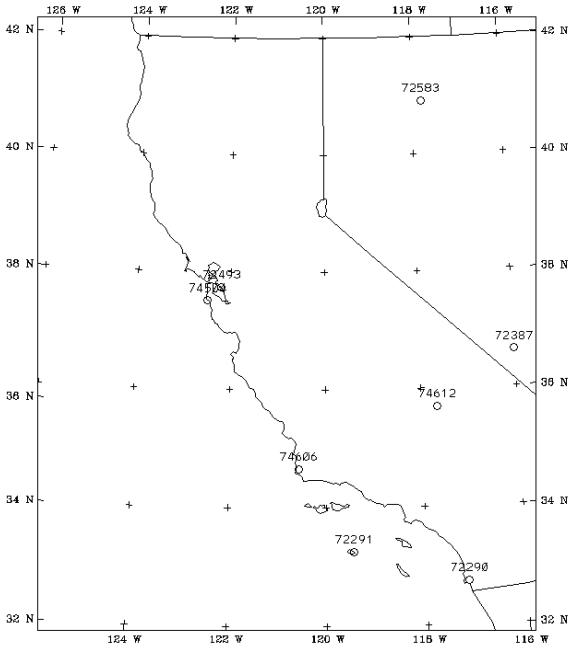

Fig. 1. Geographical location of the analyzed domain.

In the first step, we prepared a one month atmospheric simulation for July 2001, using standard satellite-based sea surface temperature data updated every 5 days. An example of the time series of the standard SST used by MM5 and measured by buoy D090 located in the Bodega Bay is presented in Fig. 2. As can be seen, the

discrepancies between the MM5 input and the buoy data are significant and reach in some cases even 4˚C. The characteristic cooling and warming periods evident in the buoy data and associated with upwelling and relaxation do not have a representation in the satellite sea surface temperature data used as an input for the atmospheric model. Therefore, the SST fields used as a standard MM5 input can not be used for precise evaluation of the atmospheric stability. As a consequence, this limitation makes precise evaluation of the stability corrected wind stress impossible and limits the available wind stress computation methods to the simple bulk formula.

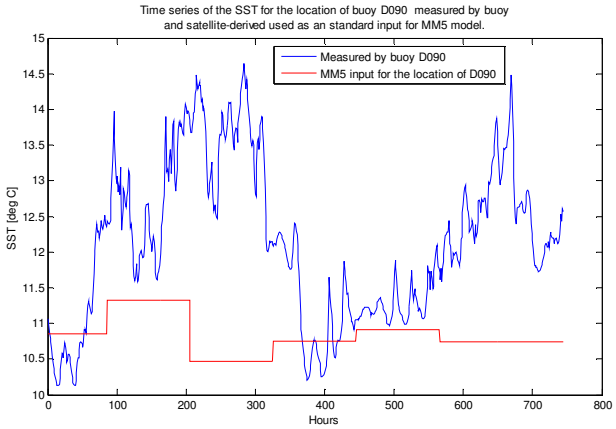

Fig. 2. Time series of the SST measured by buoy D090 and extracted from the MM5 input for this location.

In order to get more accurate sea surface temperature data that would allow us to compute the stability-corrected wind stress, and to investigate the effects of the stability induced wind stress variations on the ocean dynamics, we used the POM ocean model. The ocean model temperature field was initialized based on the NOAA GOES Imager SST and the Advanced Very High Resolution Radiometer – AVHRR data. The former, provided pure high resolution SST, but only in cloud-free areas. The latter gave full data sets but only by the virtue of advanced filtering and overlaying the measurement data with climatological datasets. Combining these two datasets provided the required SST data in 12 hour intervals, giving additional information about what part of the data came from measurements and what part was artificially prepared based on climatological datasets. Since in most cases the area of interest was cloud-free, the initial SST field was prepared by overlying these two products. As the result the final data set contained unfiltered GOES measurement data where available, filed-up by the filtered and climatologically adjusted data from AVHRR. In order to focus on the local scale effects we used radiation open boundary conditions, and assumed a uniform initial salinity field. The POM model was forced by the MM5 derived wind stress based on the Large and Pond formula for the period of one month, assuming the rest state at the beginning of the simulation.

3. VERIFICATION OF THE MODEL RESULTS

The results obtained from the atmospheric as well as ocean model were verified by comparison with buoy data for the area of Bodega Bay. For the verification of the MM5 results we focused on the wind speed simulated by the model and measured by the buoy.

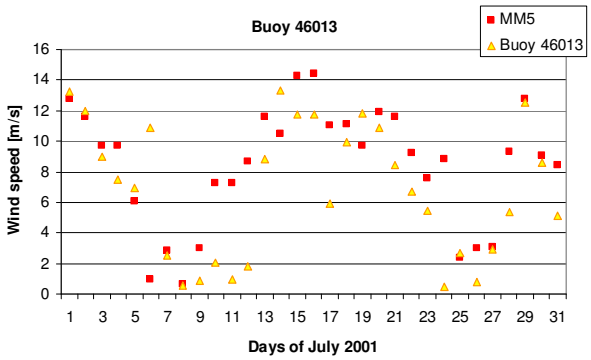

Fig. 3.Time series of daily averaged wind speed measured by buoy 46013 and simulated by MM5.

An example of a wind speed time series simulated by MM5 and measured by the buoy is presented in Fig. 3. As can be noted, the model results correlate well with the measurements. The correlation coefficient between the simulated and measured wind speed was in this case 0.7.

Since in our study we were interested in the atmospheric stability and its influence on the wind stress, wind stress curl and the upwelling velocities, the SST simulated by the POM was absolutely crucial for further analysis. Therefore, we also compared the POM-simulated SST with the results from buoys C090, D090 and E090 located in Bodega Bay. Additionally, we also verified the spatial SST picture by comparison with the GOES data. The daily averaged POM-simulated sea surface temperature shows good agreement with the measurements. The correlation coefficients for the analyzed Bodega Bay buoys were equal to 0.75, 0.7 and 0.64 respectively, with the mean error below 0.6˚C (see Fig. 4). The comparison between the simulated SST pattern at the end of the simulation period and the satellite-derived pattern also confirmed

that the modeled sea surface temperature closely agrees with the observations.

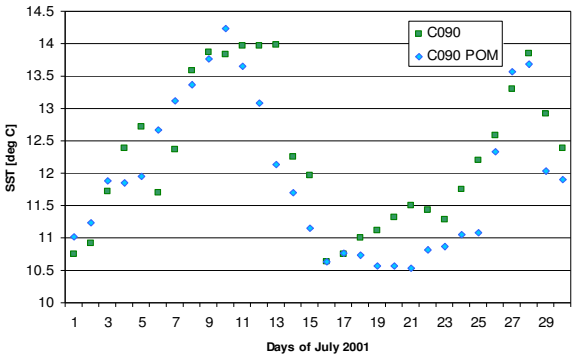

Fig. 4. Sea surface temperature measured by buoy C090 and simulated by POM.

4. THE INFLUENCE OF THE STABILITY ON THE WIND STRESS

The wind stress is of great importance to generation of upwelling. Therefore, we started from the analysis of changes in the estimated wind stress being a result of the introduction of the atmospheric stability effect on in the wind stress computation. As a base line, the wind stress computed from MM5 wind speed and the Large and Pond formula was used. In the second stage, the wind stress was computed based on the TOGA-COARE algorithm. In this case, the wind stress computation is based on the MM5-simulated wind speed, air temperature, humidity, radiation fluxes, atmospheric boundary layer height and the sea surface temperature obtained from the POM model. The comparison between the mean wind stress computed for neutral conditions using the Large and Pond formula, and the one computed according to the TOGA-COARE algorithm (taking into account the atmospheric stability effect) is presented in Fig. 5. Even though the general wind stress patterns for both cases are similar, some differences can be observed. First of all, for the northern part of the analyzed domain, north of Point Arena, the stability-corrected wind stress is significantly higher than the neutral one. As can be seen on the panel b), the TOGA-COARE-computed wind stress in this area is about 15% higher than the neutral one. This difference is the result of two factors. First, the atmosphere in this area is mostly unstable (see Fig.6). The sea surface is warmer than the air in this case, which reduces stability and enhances momentum transfer from the air to the sea, which results in an increase in the wind stress. Second, the northern part of the analyzed domain, north of Point Arena, experiences very strong wind associated with the expansion fan (Koracin and Dorman 2001, Koracin et al. 2004). The computational characteristic of the TOGA-COARE algorithm, causes the stability corrected wind stress to be significantly higher than the one from Large and Pond formula, for winds over 9 m/s (Kochanski et al. 2006), and that produces the effect observed in Fig.6.

a)

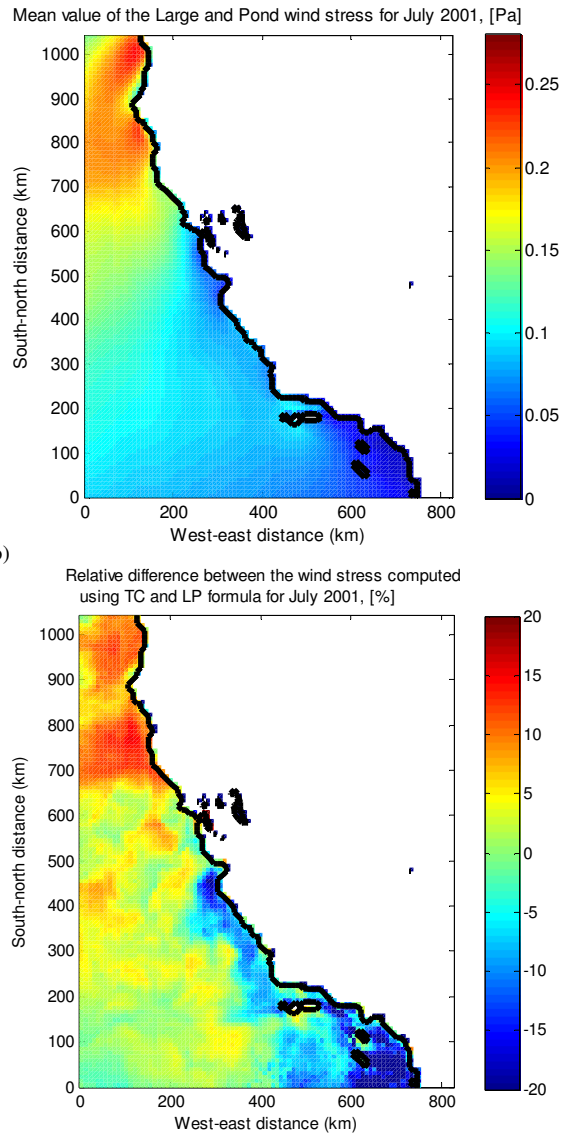

Fig. 5. The effect of stability on the wind stress, a) neutral wind stress computed form Large and Pond formula, b) percent difference between TOGA-COARE and Large and Pond wind stress.

The bias between the neutral and stability-corrected wind stress, presented in Fig.5 b, has a

complicated pattern as a result of the influence of the wind speed as well as the atmospheric stability presented in Fig.6 a. One of interesting features apparent on this graph is the band of less pronounced wind stress difference west of Cape Mendocino. This area of lower bias between neutral and stability-corrected wind stress is the result of a characteristic filament of cold water (apparent in Fig.6 panel b), upwelled at the coast over Point Mendocino, and moved off-shore by Ekman transport. This band of deep water brought to the surface significantly reduces the atmospheric stability, making the stability-corrected stress lower, and closer to the neutral one.

a)

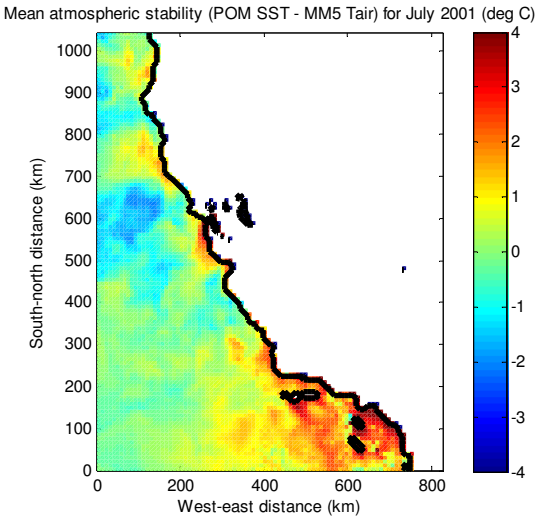

b)

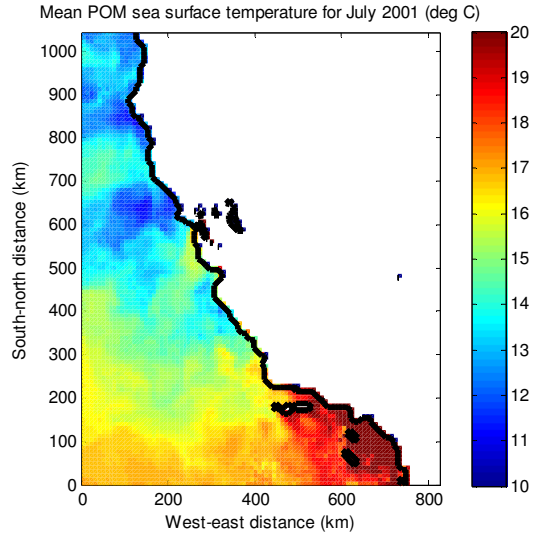

Fig. 6. Mean atmospheric stability for July 2001 - panel a) and the mean sea surface temperature for July 2001 - panel b).

More southward from Cape Mendocino, in the area of Bodega Bay, there is the area where the negative effect of increased stability makes the neutral and stability-corrected stress practically equal. This is mostly the result of the upwelling favorable winds over this area leading to a significant decrease in the SST during upwelling events (Dever et. al 2006). This cooling effect increases atmospheric stability, reducing the stability-corrected stress.

Surprisingly, the southern part of the coastal area, where unstable conditions are dominant during the month of July, experiences stability-corrected stress around 10% lower than the neutral one. This is more the result of the significant decrease of the wind speed south of the Monterey Bay than the stability effect by itself. For the wind speed in the range from 4 to 8 $m \cdot s^{-1}$, the TOGA-COARE algorithm provides significantly lower wind stress than the neutral one, computed from the Large and Pond formula. This is the result of the parabolic equation describing the roughness length, and this effect overwhelms the effect of atmospheric stability (Kochanski et. al 2006).

5. THE INFLUENCE OF THE STABILITY ON AND THE WIND STRESS CURL

Our analysis began from the wind stress alone, because its spatial variation leads to wind stress curl variability. As discussed before, the patterns of the wind stress for neutral and non-neutral cases are basically similar with relative differences below 20%. However, the patterns of the wind stress curl differ significantly – see Fig.7. The ranges of computed curl for both cases are similar, but stability-corrected wind stress curl exhibits higher variability and, evidently, more spots of strongly negative curl. For the Large and Pond wind stress curl, presented in Fig.7 a), a negative gradient of the wind stress curl in the off-shore direction can be observed along the whole coast, except for the 40km spot south of Cape Mendocino and approximately 150 km segment between Big Sur and Moro Bay, where persistent strong winds at the Santa Lucia mountain range interacting with weaker winds off-shore induce persistent negative curl. Over the rest of the coast, there is a band of strong mean positive curl up to 0.15 Pa/100km, vanishing off-shore, and split by two north-south oriented bands of weaker curl evident between Cape Mendocino and Monterey Bay.

The stability-corrected wind stress curl exhibits a much more complex picture. First of all,

the band of the strong positive curl evident in the neutral case (Fig.8. panel a) is split by extensive negative curl located north of an area of Point Mendocino. The main reason for that is the slight enhancement of the wind stress in the band of strong wind near the shore and wind stress reduction at the west side of the domain. This nonlinear enhancement of the wind stress promotes more negative curl than observed for the neutral wind stress curl.

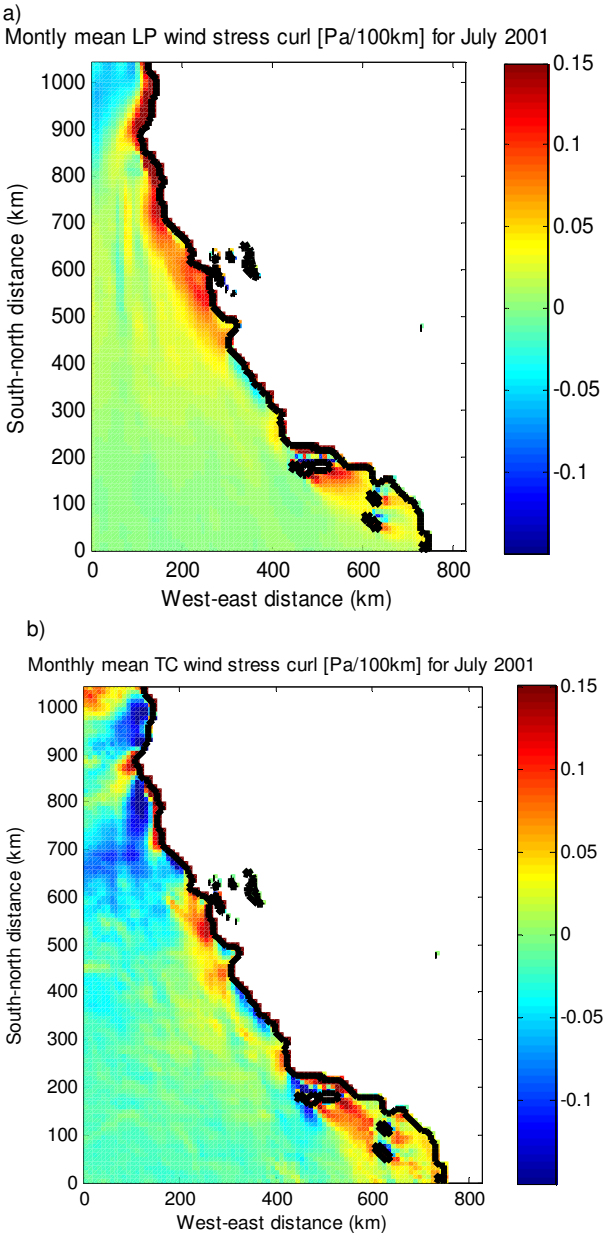

Fig. 7. Comparison between the monthly mean of the wind stress curl for July 2001, a) neutral case, and b) curl of stability-corrected wind stress.

Additionally, the stability effect plays a role in differentiating the east-west wind stress component. The filament of cold water evident in Fig. 6b, west of Cape Mendocino, enhances stability and reduces the wind stress over this area, which increases the curl in its vicinity, and reduces the curl to the south down to the San Francisco Bay.

In this part of our domain, spreading southward, down to Point Arena, for the stability-corrected wind stress, the positive curl is confined to a very narrow coastal band and becomes strongly negative just 20 km off-shore. The most pronounced positive spots in this part of the domain are located at Cape Mendocino and Point Arena, while for the neutral case, there is a uniform positive wind stress curl band ending at Point Sur. The locations of these spots correspond to the rapid changes in stability observed in Fig.6a. A very interesting feature can be noticed in vicinity of Bodega Bay and southward down to Monterey Bay. Bodega Bay seems to be exactly at the boundary between the areas where stability reduces and enhances wind stress curl. The mean winds in this area are around 6-7 m/s, while more westward, the wind is much stronger reaching 10 m/s. For the Large and Pond formula, below 11 m/s the drag coefficient is constant, and increases linearly above this value. Therefore the wind stress curl computed based on this formula is significantly reduced in comparison to TOGA-COARE algorithm, for which the difference in the drag coefficient and wind stress between 7 and 10 m/s is significantly greater.

5. THE EFFECT OF STABILITY ON THE UPWELLING

The wind stress curl is one of the main factors controlling the upwelling process. The analysis presented in the previous section showed pronounced difference in the wind stress curl pattern as a result of introducing of more sophisticated algorithm, taking into account the effect of stability, in the wind stress computation. Now, we would like to examine what is the effect of these differences on the ocean response, and whether introduction of the stability in to the wind stress computation significantly affects the ocean response. In order to perform this analysis, we run the POM model again, but this time we forced it with stability corrected wind stress. The comparison between the simulated upwelling velocities for the neutral and stability-corrected wind stress is presented in Fig.7. Both series

presented in Fig.7 show mostly upward velocities corresponding to the upwelling events. However, the introduction of stability in the wind stress computation significantly enhances the simulated upwelling velocity. The monthly mean value for the run with stability-corrected wind stress is around twice the magnitude of the one from the run with the neutral stress ($1.3 \cdot 10^{-5}$ m·s^{-1} vs. $5.7 \cdot 10^{-6}$ m·s^{-1}).

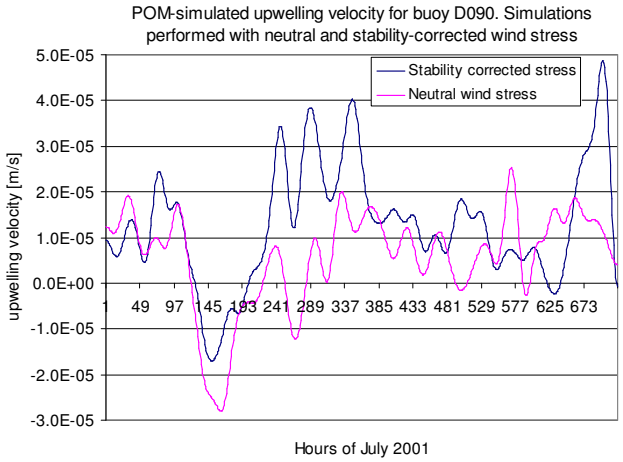

Fig.7. Time series of the 38h low-pass filtered POM-simulated upwelling velocities for a case of neutral (Large and Pond) wind stress (pink line), and stability corrected wind stress - TOGA-COARE (navy line).

Also, the variations in the upwelling velocity simulated for stability corrected wind stress is around 25% greater for the run with the TOGA-COARE wind stress than for the one with the Large and Pond stress. A closer look at the upwelling velocity time series reveals also that the upwelling and relaxation periods are more pronounced in the POM run forced by the stability corrected stress than for the one forced by the neutral stress. For the latter case, upwelling velocity fluctuations do not show pronounced upwelling and relaxation periods. For the second part of the month, vertical velocity oscillates with a frequency of around 48 hours without evident indication of upwelling and relaxation events. The results obtained after the introduction of stability to the wind stress computation significantly improve the upward velocity variations, which now show the three characteristic June upwelling events observed during the WEST experiment. This result shows that the atmospheric stability, even if it doesn't change the wind stress dramatically, leads to changes in the wind stress curl strong enough to have a pronounce effect on the computed upwelling velocity. Of course, a further study including detailed comparison of the POM simulated upwelling with measurements are required to verify if this change in model forcing leads to improvement of ocean model results.

6. ACKNOWLEDGEMENT

The study has been supported by NSF EPSCOR. The authors would like to thank Ed Dever for providing the low-pass data filter used in this study.

References

Dever, E.P., Dorman, C.E., Largier, J.L., 2006. Surface boundary layer variability off northern California, USA during upwelling. *Deep-Sea Research II*, **53** (2006) 2887–2905.

Fairall, C.W., Bradley, E.F., Rogers, D.P., Edson, J.B., Young, G.S., 1996. Bulk parameterization of air-sea fluxes for Tropical Ocean Global Atmosphere Coupled Ocean-Atmosphere Response Experiment. *Journal of Geophysical Research* **101**, 3747-3764.

Fairall, C.W., Bradley, E.F., Godfrey,J.S., Wick, G.A., Edson, J.B., Young, G.S., 1996. Cool-Skin and warm-layer effects on sea surface temperature. *Journal of Geophysical Research* **101**, 1295-1308.

Kochanski, A., D. Koracin, C. E. Dorman, 2006: Comparison of wind-stress algorithms and their influence on wind-stress curl using buoy measurements over the shelf off Bodega Bay, California, *Deep-Sea Research II* **53** (2006) 2865–2886

Koracin, D., C. E. Dorman, and E. P. Dever, 2004: Coastal perturbations of marine layer winds, wind stress, and wind stress curl along California and Baja California in June 1999. *J. Phys. Ocean.*, **34**, 1152-1173.

Koracin, D., Dorman, C.E., 2001. Marine atmospheric boundary layer divergence and clouds along California in June 1996. *Monthly Weather Review* **129**, 2040–2056.

Large, W. G., and S. Pond, 1981: Open ocean momentum flux measurements in moderate to strong winds. *J. Phys. Ocean*, **11**, 324-481.